Circular orbits of charged particles around a weakly charged and magnetized Schwarzschild black hole

A. M. Al Zahrani◉*

Physics Department, King Fahd University of Petroleum and Minerals, Dhahran 31261, Saudi Arabia

We study the circular orbits of charged particles around a weakly charged Schwarzschild black hole immersed in a weak, axisymmetric magnetic field. We start by reviewing the circular orbits of neutral particles and charged particles around only weakly charged and only weakly magnetized black holes. The case of a weakly magnetized and charged black hole is investigated then. In particular, we study the effect of the electromagnetic forces on the charged particle innermost stable circular orbits. We show that negative energy stable circular orbits are possible and that two bands of charged particles circular orbits, separated by a gap of no stable circular orbits can exist. The astrophysical aspects of our findings are discussed too.

I. INTRODUCTION

Black hole astrophysics has been one of the most intriguing disciplines of science. It reached the pinnacle of fascination when the first real image of a black hole was published by the Event Horizon Telescope Collaboration. One of the principal objectives of black hole astrophysics is to measure the parameters of a black hole, in particular, its mass and spin angular momentum. According to the no-hair theorem, a stationary black hole is characterized by only three parameters: mass, spin angular momentum, and charge [1]. It has been argued that astrophysical black holes are indeed electrically neutral. If some excess charge is produced by whatever astrophysical processes, it would be shortly neutralized by the selective accretion of the ambient plasma. The wide adoption of this assumption can be explicitly seen in the literature where charged black holes are hardly considered, except for academic purposes.

There are several profound reasons to assume that weakly charged black holes exist, however. The mass difference between electrons and protons may render a black hole positively charged (see Refs. [2–4], and the references within). Moreover, a rotating black hole immersed into a homogeneous magnetic field acquires a nonvanishing electrical field. This can result in the selective accretion of the ambient, free charged particles, until the black hole's charge neutralizes the magnetically induced electric field [5,6]. Another effect that might charge a black hole is the difference in the accretion rates of electrons and protons of the surrounding plasma in the presence of radiation from the accreting matter.

It is widely accepted that astrophysical black holes are magnetized. The main source of the magnetic fields is the plasma in the accretion disk as discussed in Refs. [7,8]. In addition to the theoretical considerations, there are abundant observational data that back this assertion [9–13].

The innermost stable circular orbit (ISCO) of a black hole has several immediate implications. It is vital for measuring the spin angular momentum of the black hole [14]. It is also influential to the structure of the accretion disk [15]. For an accretion disk with low luminosity compared to the Eddington luminosity, the ISCO coincides with the inner edge of the disk [16]. Therefore, the ISCO has a direct impact on the structure of the black hole's shadow.

The charged particle ISCOs around a Schwarzschild and Kerr black holes immersed in a weak, axially symmetric magnetic field were extensively investigated [17–20]. In all cases, the effect of the magnetic field is to bring the ISCO closer to the black hole. The dynamics of charged particles in Reissner-Nordstrom spacetime was investigated in [21,22]. The charged particles ISCOs around a weakly charged Schwarzschild black hole were addressed in [2–4]. The combined affects of the magnetic field and black hole's charge on the ISCOs have been recently examined in Ref. [23] for a few special cases.

In this paper we study the ISCOs of charged particles orbiting a Schwarzschild black hole that is weakly charged and immersed in a weak, axisymmetric magnetic field. The black hole's charge and magnetic field are weak in the sense that their backreactions on the spacetime are insignificant.[1] We first look at the effect of each of the magnetic field and black hole's charge separately and then study their combined effect. We explore in detail the cases when no

---

*amz@kfupm.edu.sa; ama3@ualberta.ca

[1]In what follows, it should be inferred that the black hole's charge and magnetic field are assumed to be weak.

ISCO exists and when the particle's energy becomes negative. The paper is organized as follows: Sec. II is a review of the circular orbits and the ISCO of a neutral particle. In Sec. III, we go over the Wald solution of Maxwell's equations in Ricci flat spacetimes and write the radial equation of motion for a charged test particle. In Secs. IV and V we discuss the ISCOs of a charged particle near a charged black hole and magnetized black hole, respectively. In Sec. VI, we investigate in detail the charged particle ISCOs near a charged black hole immersed in a magnetic field. General discussion and conclusion are given in Sec. VII. We use the sign conventions adopted in Ref. [1] and geometrized units where c, G and k (the Coulomb constant) are unity.

II. CIRCULAR ORBITS OF A NEUTRAL PARTICLE AROUND A SCHWARZSCHILD BLACK HOLE

The spacetime geometry around a spherically symmetric black hole of mass M is described by the Schwarzschild metric, which reads [1]

$$ds^2 = -f(r)dt^2 + \frac{dr^2}{f(r)} + r^2 d\theta^2 + r^2\sin^2\theta d\phi^2, \quad (1)$$

where

$$f(r) = 1 - \frac{2M}{r}. \quad (2)$$

The Schwarzschild metric admits four Killing vectors. Two of them are the temporal and azimuthal Killing vectors, since the metric is temporally and azimuthally symmetric. They read, respectively,

$$\xi^\mu_{(t)} = \delta^\mu_t, \qquad \xi^\mu_{(\phi)} = \delta^\mu_\phi. \quad (3)$$

Let a test particle of mass m be moving with four-velocity u^μ in the Schwarzschild background. There are two constants of the particle's motion associated with the two Killing symmetries:

$$\mathcal{E} = -p_\mu \xi^\mu_{(t)}/m = f(r)\dot{t}, \quad (4)$$

$$\mathcal{L} = p_\mu \xi^\mu_{(\phi)}/m = r^2\sin^2\theta\dot{\phi}. \quad (5)$$

Here $p^\mu = mu^\mu$ is the particle's four-momentum. The two constants of motion $\mathcal{E}$ and $\mathcal{L}$ are the specific energy and specific azimuthal angular momentum, respectively. Using them along with the normalization $u_\mu u^\mu = -1$, we reduce the radial equation of motion in the equatorial submanifold ($\theta = \pi/2$, $\dot{\theta} = 0$) to quadrature:

$$\dot{r}^2 = \mathcal{E}^2 - V(r). \quad (6)$$

The overdot denotes differentiation with respect to the particle's proper time. The effective potential $V(r)$ reads

$$V(r) = \left(1 - \frac{\mathcal{L}^2}{r^2}\right)f(r). \quad (7)$$

The radial motion is invariant under the transformations

$$\phi \to -\phi, \qquad \dot{\phi} \to -\dot{\phi}, \qquad \mathcal{L} \to -\mathcal{L}. \quad (8)$$

Therefore, there is only one mode of radial motion. Without loss of generality, we will consider $\mathcal{L} > 0$.

The two conditions of circular motion $V(r) = \mathcal{E}$ and $V'(r) = 0$ give us

$$\mathcal{E}^2 = \left(1 - \frac{\mathcal{L}^2}{r^2}\right)f(r), \quad (9)$$

$$\mathcal{E}^2(r - M) + (2r - 3M)r^2 = 0. \quad (10)$$

We will use r_o, $\mathcal{E}_o$ and $\mathcal{L}_o$ to denote quantities corresponding to circular orbits from here on. Solving the above two equations for $\mathcal{E}_o$ and $\mathcal{L}_o$ for future-directed orbits yields

$$\mathcal{E}_o = \frac{(r_o - 2M)}{r_o^{1/2}\sqrt{r_o - 3M}}, \quad (11)$$

$$\mathcal{L}_o = \frac{Mr_o}{\sqrt{r_o - 3M}}. \quad (12)$$

The value of $\mathcal{E}_o$ is always positive with a value of 1 far away from the black hole. A circular orbit is the ISCO when $V''(r_o)$ vanishes. This condition gives us that $r_{\text{ISCO}} = 6M$. It is worth mentioning that $\mathcal{E}_{\text{ISCO}} = 2\sqrt{2}/3$ and $\mathcal{L}_{\text{ISCO}} = 2\sqrt{3}M$. Therefore, a particle ending in the ISCO can release an energy of $1 - 2\sqrt{2}/3(\approx 0.057)$ of its rest energy.

III. CHARGED AND MAGNETIZED SCHWARZSCHILD BLACK HOLES

Let us now review Wald's solution of Maxwell equations in a curved spacetime for weak electromagnetic fields [6]. In a Ricci flat spacetime a Killing vector ξ^μ obeys the equation

$$\xi^\mu{}_{;\nu}{}^{;\nu} = 0. \quad (13)$$

This is identical to the source-free Maxwell equations for a four-potential A^μ in the Lorentz gauge ($A^\mu{}_{;\mu} = 0$):

$$A^\mu{}_{;\nu}{}^{;\nu} = 0. \quad (14)$$

Therefore, any linear combination of the Killing vectors the spacetime admits is automatically a solution to the Maxwell equations.

Consider the electromagnetic potential constructed of the temporal and azimuthal Killing vectors of the Schwarzschild geometry:

$$A^\mu = -\frac{Q}{2M}\xi^\mu_{(t)} + \frac{B}{2}\xi^\mu_{(\phi)}. \tag{15}$$

Lowering the index and removing the constant term give

$$A_\mu = -\frac{Q}{r}\delta^t_\mu + \frac{B}{2}r^2\sin^2\theta\delta^\phi_\mu. \tag{16}$$

This potential describes the electromagnetic fields around a charged black hole immersed in an axisymmetric magnetic field. The black hole's charge Q is given by

$$Q = \frac{1}{4\pi}\int_\sigma F^{\mu\nu}d\sigma_{\mu\nu}, \tag{17}$$

where σ is a 2D surface surrounding the black hole and $F^{\mu\nu}$ is the electromagnetic field tensor [see Eq. (19)]. The magnetic field is axisymmetric with a strength of B asymptotically [6,18,19]. This is the potential that we will use in this paper.

The dynamics of a charged particle of mass m and charge e in an electromagnetic field in a curved spacetime is governed by the equation

$$mu^\nu\nabla_\nu u^\mu = eF^\mu_{\ \rho}u^\rho. \tag{18}$$

The electromagnetic field tensor $F^\mu_{\ \nu}$ is given by

$$F_{\mu\nu} = A_{\nu,\mu} - A_{\mu,\nu}. \tag{19}$$

In the frame of an observer with four-velocity u^{obs}_μ, the electric and magnetic fields are, respectively,

$$E^i = F^{i\nu}u^{obs}_\nu, \tag{20}$$

$$B^i = \frac{1}{2}\frac{\varepsilon^{i\nu\lambda\sigma}}{\sqrt{-g}}F_{\lambda\sigma}u^{obs}_\nu, \tag{21}$$

where $g = \det(g_{\mu\nu})$, $\varepsilon_{0123} = +1$ and $i = 1, 2, 3$.

For a stationary observer ($u^{obs}_\mu = -f^{1/2}\delta^t_\mu$), the electric and magnetic field are, respectively,

$$E^i = \frac{Qf^{1/2}}{r^2}\delta^i_r, \tag{22}$$

$$B^i = Bf^{1/2}\left(\cos\theta\delta^i_r - \frac{\sin\theta}{r}\delta^i_\theta\right). \tag{23}$$

The generalized four-momentum of the particle is

$$P_\mu = mu_\mu + eA_\mu. \tag{24}$$

The Lie derivatives of A_μ with respect to $\xi^\mu_{(t)}$ and $\xi^\mu_{(\phi)}$ identically vanish:

$$\mathcal{L}_{\xi^\nu_{(t)}}A^\mu = 0, \tag{25}$$

$$\mathcal{L}_{\xi^\nu_{(\phi)}}A^\mu = 0. \tag{26}$$

The energy and azimuthal angular momentum of a charged particle are therefore constants of motion. Equations (4) and (5) are generalized to

$$\mathcal{E} = -P_\mu\xi^\mu_{(t)}/m = \frac{q}{r} + f(r)\dot{t}, \tag{27}$$

$$\mathcal{L} = P_\mu\xi^\mu_{(\phi)}/m = r^2(b + \dot\phi)\sin^2\theta, \tag{28}$$

respectively, where $q = eQ/m$ and $b = eB/2m$. We can straightforwardly obtain the charged particle version of Eq. (6) by combining Eqs. (27) and (28) with $u_\mu u^\mu = -1$. The radial equation of motion in the equatorial submanifold then reads

$$r^2\dot{r}^2 = (\mathcal{E}r - q)^2 - [r^2 + (\mathcal{L} - br^2)^2]f(r). \tag{29}$$

It is more convenient to recast it as

$$\dot{r}^2 = (\mathcal{E} - V_+)(\mathcal{E} - V_-), \tag{30}$$

where

$$V_\pm(r) = \frac{q}{r} \pm \sqrt{\left[1 + \left(\frac{\mathcal{L}}{r} - br\right)^2\right]f(r)}. \tag{31}$$

It is $V_+(r)$ that corresponds to future-directed orbits. Equation (29) is invariant under the symmetry transformations

$$\phi \to -\phi, \quad \dot\phi \to -\dot\phi, \quad \mathcal{L} \to -\mathcal{L}, \quad b \to -b. \tag{32}$$

As in the previous section, we will keep $\mathcal{L} > 0$ without any loss of generality. When $b > 0$ ($b < 0$), the magnetic force is radially out (in). Likewise, $q > 0$ ($q < 0$) corresponds to Coulomb repulsion (attraction). Therefore, there are four different modes of radial motion, in general.

The weak field approximation breaks down when the electric charge and magnetic field creates curvatures comparable to that made by the black hole's mass near the event horizon. This happens when

$$B^2 \sim M^{-2} \quad \text{or} \quad Q^2 \sim M^2. \tag{33}$$

In conventional units, the weak field approximation fails when

$$Q \sim \frac{G^{1/2}M}{k^{1/2}} \sim 10^{20} \frac{M}{M_\odot} \text{ C} \qquad (34)$$

or

$$B \sim \frac{k^{1/2}c^3}{G^{3/2}M} \sim 10^{19} \frac{M_\odot}{M} \text{ G}, \qquad (35)$$

where $M_\odot$ is the solar mass.

The typical magnetic field strength near a black hole's horizon has been estimated to be $\sim 10^8$ G (10^{-15} m^{-1}) for stellar mass black holes and $\sim 10^4$ G (10^{-19} m^{-1}) for supermassive black holes [9–13]. According to Ref. [3], the charge of Sgr A* is estimated to be in the range 10^8–10^{15} C (10^{-9}–10^{-2} m). These estimates validate ignoring corrections to the metric due to the presence of the electromagnetic fields.

In spite of the fact that the electromagnetic fields are geometrically insignificant, their effects on the dynamics of charged particles can be significant since $e/m = 2.04 \times 10^{21}$ (1.11×10^{18}) for electrons (protons). For electrons and protons near a black hole with $Q = 10^8$ C and $B = 10^4$ G, for example,

$$q_e \sim 10^{12} \text{ m}, \qquad q_p \sim 10^9 \text{ m}, \qquad (36)$$

and

$$b_e \sim 10^3 \text{ m}^{-1}, \qquad b_p \sim 10^{-1} \text{ m}^{-1}. \qquad (37)$$

The subscripts "e" and "p" refer to electrons and protons, respectively.

IV. CIRCULAR ORBITS AROUND A CHARGED SCHWARZSCHILD BLACK HOLE

Now, we write the expressions similar to Eqs. (11) and (12) for a charged particle orbiting a charged Schwarzschild black hole and study its circular orbits and ISCOs. Setting $b = 0$ in Eq. (31) gives

$$V_+(r) = \frac{q}{r} + \sqrt{\left(1 + \frac{\mathcal{L}^2}{r^2}\right)\left(1 - \frac{2M}{r}\right)}. \qquad (38)$$

The two conditions for circular orbits [$V(r) = \mathcal{E}$ and $V'(r) = 0$] yield, respectively,

$$\mathcal{E}_o = \frac{q}{r_o} + \sqrt{\left(1 + \frac{\mathcal{L}_o^2}{r_o^2}\right)\left(1 - \frac{2M}{r_o}\right)} \qquad (39)$$

and

$$\mathcal{L}_o^2 = \frac{2Mr_o^2}{r_o - 3M} + \left[\frac{qr_o(r_o - 2M)}{(r_o - 3M)^2}\right.$$
$$\left. \times (q - \sqrt{4r_o(r_o - 3M) + q^2})\right]. \qquad (40)$$

The condition for a circular orbit to be the ISCO $V''(r_o) = 0$ reads

$$[r_o(\mathcal{L}_o^2 + r_o^2)(r_o - 2M)]^{1/2}(\mathcal{L}_o^2 - 2Mr_o)$$
$$+ q[\mathcal{L}_o^2(r_o - M) + r^2(2r_o - 3M)] = 0. \qquad (41)$$

Figures 1–3 show how the radius, azimuthal specific angular momentum and specific energy of the ISCO vary with q, respectively. For $q > 0$, r_{ISCO} increases very steeply and approaches infinity as q approaches M, in agreement with Refs. [2,21]. This is because the Coulomb repulsion makes the circular orbits less stable. The destabilization effect is due to the first term in Eq. (38) which creates a
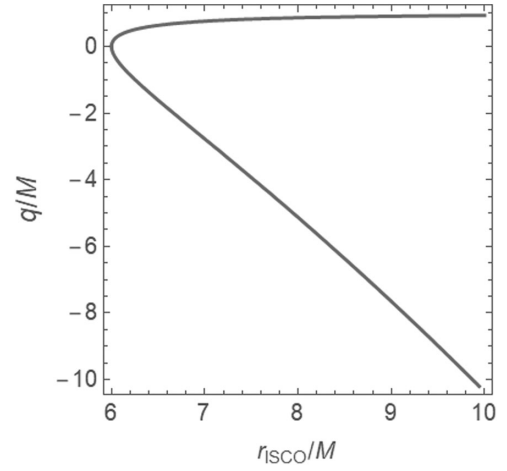

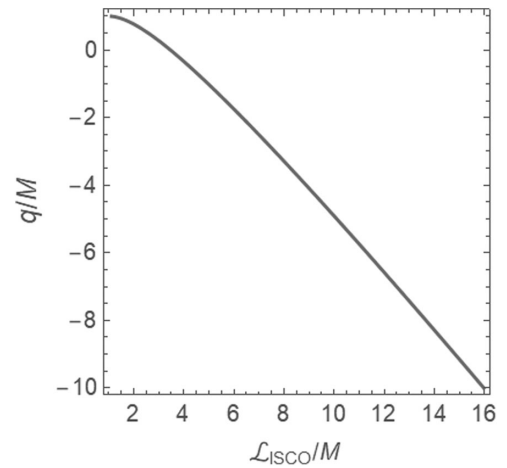FIG. 1. The radius of the ISCO versus the charge parameter q.

FIG. 2. The specific azimuthal angular of the ISCO versus the charge parameter q.
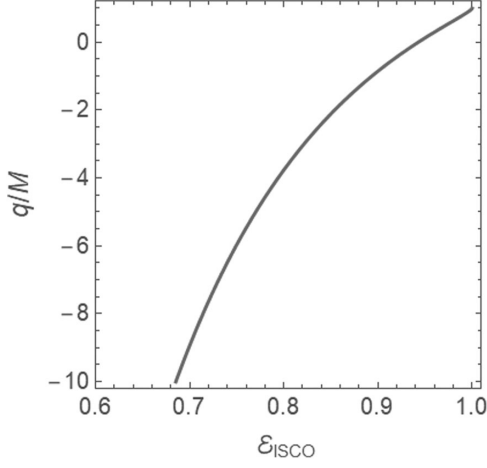
FIG. 3. The specific energy of the ISCO versus the charge parameter q.

hump in V_+ near $r = 2M$ for $q > 0$. When $q < 0$, r_{ISCO} also increases as the magnitude of q increases, but more smoothly. Overall, the black hole charge pushes away r_{ISCO} beyond $r = 6M$ for both signs of q. We can see this effect explicitly by expanding $r_{\text{ISCO}}(q)$ around $q = 0$, which yields

$$r_{\text{ISCO}} = 6M + \frac{q^2}{2M} + \mathcal{O}(q^3). \qquad (42)$$

Thus, $r_{\text{ISCO}} > 6M$ whenever $|q| > 0$.

At $q = M$, $\mathcal{L}_{\text{ISCO}}$ has its minimum of M. It then increases monotonically as q decreases. On the other hand, $\mathcal{E}_{\text{ISCO}}$ has its maximum of 1 when $q = M$. As q decreases, $\mathcal{E}_{\text{ISCO}}$ monotonically decreases and approaches 0 as q approaches $-\infty$. Therefore, the efficiency of energy liberation of a charged particle at the ISCO can be close to 100% of the particle's rest energy.

In the case when $q \ll -M$, we can write approximate expressions for r_{ISCO}, $\mathcal{L}_{\text{ISCO}}$ and $\mathcal{E}_{\text{ISCO}}$ as

$$r_{\text{ISCO}} \approx \sqrt[3]{2Mq^2}, \qquad (43)$$

$$\mathcal{L}_{\text{ISCO}} \approx -q, \qquad (44)$$

$$\mathcal{E}_{\text{ISCO}} \approx 3\sqrt[3]{-M/4q}. \qquad (45)$$

The results of this section, and the relationship between r_{ISCO} and q in particular, demonstrates that even a trace charge on a black hole can have profound astrophysical implications.

V. CIRCULAR ORBITS AROUND A MAGNETIZED SCHWARZSCHILD BLACK HOLE

In this section, we review the circular orbits and the ISCOs of a charged particle near a magnetized

Schwarzschild black hole. Equation (31) with $q = 0$ reads

$$V_+(r) = \sqrt{\left[1 + \left(\frac{\mathcal{L}}{r} - br\right)^2\right]f(r)}. \qquad (46)$$

The two conditions for circular orbits give us that

$$\mathcal{E}_o = \sqrt{\left[1 + \left(\frac{\mathcal{L}_o}{r_o} - br_o\right)^2\right]\left(1 - \frac{2M}{r_o}\right)}, \qquad (47)$$

$$\mathcal{L}_o = \frac{r_o\sqrt{b^2 r_o^2(r_o - 2M)^2 + M(r_o - 3M)}}{r_o - 3M}$$
$$- \frac{bMr_o^2}{r_o - 3M}. \qquad (48)$$

For a circular orbit to be the ISCO, it must satisfy the condition

$$b^2 r_o^3(5r_o - 4M) - 4b\mathcal{L}_o Mr - \mathcal{L}_o^2 + 2Mr_o = 0. \qquad (49)$$

Figure 4 shows r_{ISCO} versus b. The effect of the magnetic field is always to bring the ISCO inward closer than $r = 6M$. As b approaches ∞ and $-\infty$, r_{ISCO} approaches $2M$ and $(\sqrt{13} + 5)M/2$, respectively. Figures 5 and 6 show $\mathcal{L}_{\text{ISCO}}$ and $\mathcal{E}_{\text{ISCO}}$ versus b, respectively. When $b \to \infty$, $\mathcal{L}_{\text{ISCO}}$ approached ∞ but $\mathcal{E}_{\text{ISCO}}$ approach 0. The efficiency of energy release for a charged particle ending at the ISCO can be close to 100% of the particle's rest energy. As $b \to -\infty$, both $\mathcal{L}_{\text{ISCO}}$ and $\mathcal{E}_{\text{ISCO}}$ approach ∞.
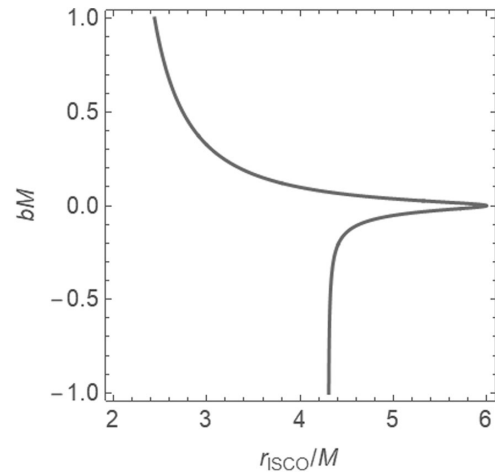

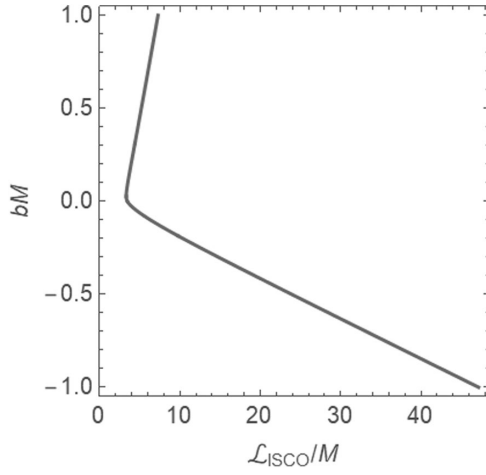FIG. 4. The radius of the ISCO versus the magnetic parameter b.

FIG. 5. The specific azimuthal angular of the ISCO versus the magnetic parameter b.
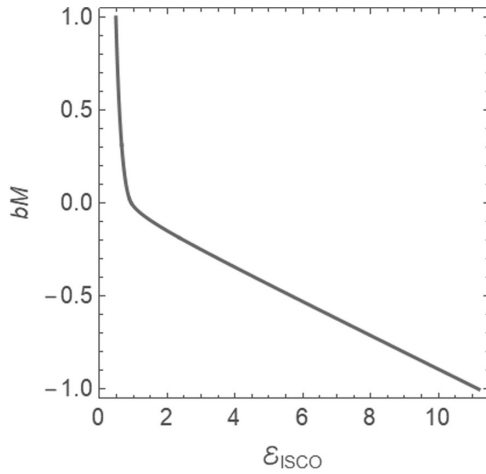

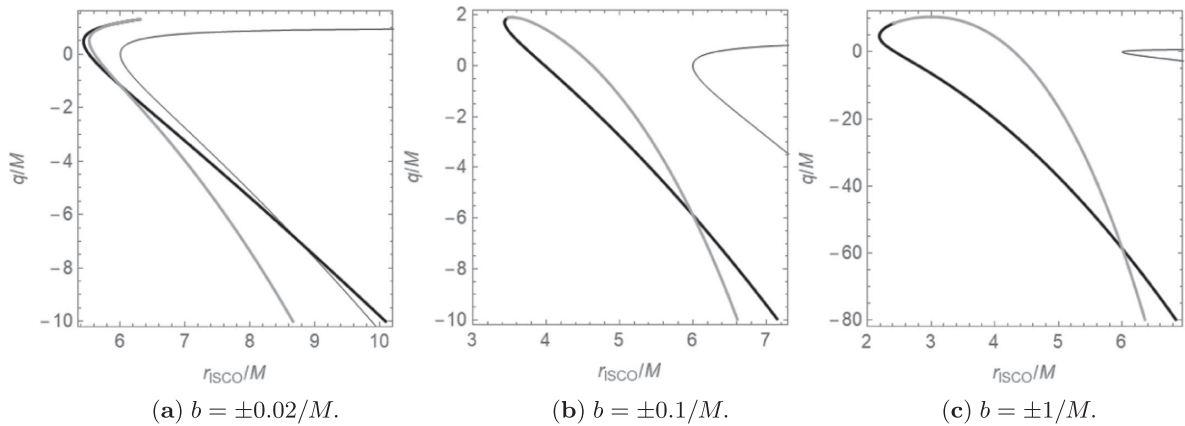FIG. 6. The specific energy of the ISCO versus the magnetic parameter b.

VI. CIRCULAR ORBITS AROUND A CHARGED AND MAGNETIZED SCHWARZSCHILD BLACK HOLE

Applying the two conditions for circular orbits to the effective potential of Eq. (31) yields

$$\mathcal{E}_o = \frac{q}{r_o} + \sqrt{\left[1 + \left(\frac{\mathcal{L}_o}{r_o} - br_o\right)^2\right]\left(1 - \frac{2M}{r_o}\right)}, \quad (50)$$

where $\mathcal{L}_o$ is determined by the equation

$$b^2 r_o^4(r_o - M) + Mr_o^2(1 - 2b\mathcal{L}_o) + \mathcal{L}_o^2(3M - r_o)$$
$$- q\sqrt{r_o(r_o - 2M)[(\mathcal{L}_o - br_o^2)^2 + r_o^2]} = 0. \quad (51)$$

While it is possible to solve this equation for $\mathcal{L}_o$ explicitly, the resulting expression is extremely cumbersome. The ISCO condition reads

$$b^2 r_o^3(5r_o - 4M) - 4b\mathcal{L}_o Mr_o - \mathcal{L}_o^2 + 2Mr_o - \frac{q}{r_o}A$$
$$- \frac{q}{A}[b^2 r_o^4(2r_o - 3M) + 2b\mathcal{L}_o r_o^2(M - r_o) + \mathcal{L}_o^2 M$$
$$+ r_o^2(r_o - M)] = 0, \quad (52)$$

where

$$A = \sqrt{r_o(r_o - 2M)[(\mathcal{L}_o - br_o^2)^2 + r_o^2]}. \quad (53)$$

In order to visualize the behavior of r_{ISCO} when both q and b are nonzero, we will reproduce Fig. 1 for selected, representative values of b. Figure 7 shows the effect of turning on the magnetic field on the r_{ISCO} versus q curve. The magnetic field has mainly three effects on r_{ISCO}: (i) It brings r_{ISCO} closer to the black hole. In all cases where $b \neq 0$, r_{ISCO} is finite. (ii) It makes $q_{\text{max}} > M$, where q_{max} is

(a) $b = \pm 0.02/M$.

(b) $b = \pm 0.1/M$.

(c) $b = \pm 1/M$.

FIG. 7. The radius of the ISCO versus q for selected values of b. The thick black (gray) curve corresponds to the positive (negative) value of b. The thin curve corresponds to $b = 0$.
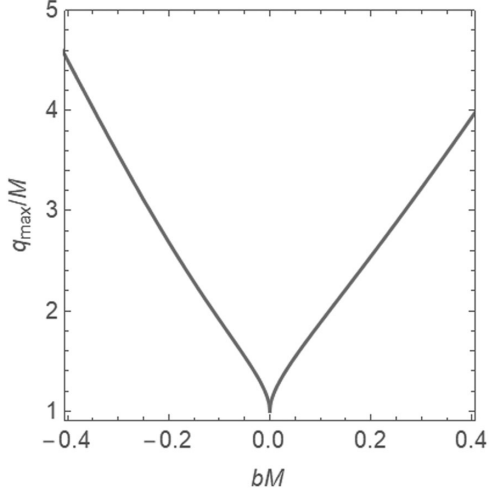
FIG. 8. The dependence of the maximum value of q at which the ISCO exists (q_{max}) on b.

the maximum possible value of q for which r_{ISCO} exists. (iii) It can creates two concurrent ISCOs when $b < 0$ (see below). These three effects become more evident as $|b|$ increases. Figure 8 shows q_{max} versus b. When $q = q_{max}$, $\mathcal{L}_{ISCO} = 0$ for $b > 0$ only. The relationship between q_{max} and b can be well approximated to be linear when $|b| \gtrsim 10^{-1}/M$ as

$$q_{max} \approx 8.22bM^2 \qquad (b \gtrsim 10^{-1}/M), \qquad (54)$$

$$q_{max} \approx -10.4bM^2 \qquad (b \lesssim -10^{-1}/M). \qquad (55)$$

When both q and b are very large and positive ($q \gg M$, $b \gg 1/M$), r_{ISCO} approaches $[(3 + \sqrt{3})/2]M \approx 2.366M$ and q_{max} approaches $(\sqrt{135 + 78\sqrt{3}}/2)bM^2 \approx 8.217bM^2$. However, when q and $|b|$ are very large, q is positive, but b is negative ($q \gg M$, $b \ll -1/M$), r_{ISCO} approaches $3M$ and q_{max} approaches $-6\sqrt{3}bM^2 \approx -10.39bM^2$.

We can see in the three plots of Fig. 7 that the positive b and negative b curves always cross at $r_{ISCO} = 6M$, the neutral particle value. This finding was noted in Ref. [23]. It may be tempting to think that the radial component of the electromagnetic force ($eF^r{}_\rho u^\rho$) vanishes where the crossing occurs, but this is not the case. The corresponding values of $\mathcal{L}_{ISCO}$ and $\mathcal{E}_{ISCO}$ are different from the neutral particle values.

The most interesting finding is the occurrence of an inner and outer ISCOs when $b < 0$. This happens when the charge parameter is in the interval $q_{max}(|b|) < q < q_{max}(-|b|)$. The coexistence of the two ISCOs implies the existence of a forbidden zone where stable circular orbits of charged particles cannot exist. The outer boundary of the forbidden zone is the outer ISCO. The inner boundary is the circular orbit at $r_o|_{\mathcal{L}_o=0}$, the value of r_o
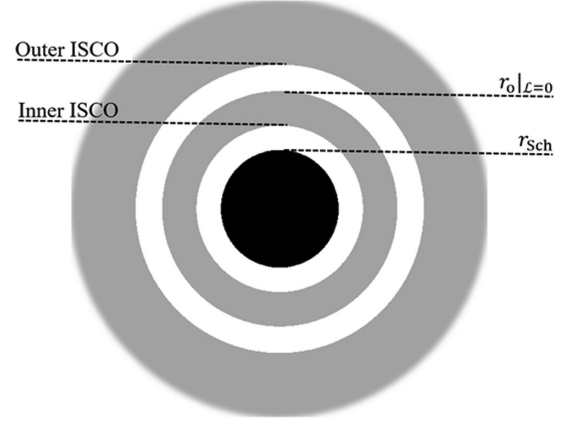

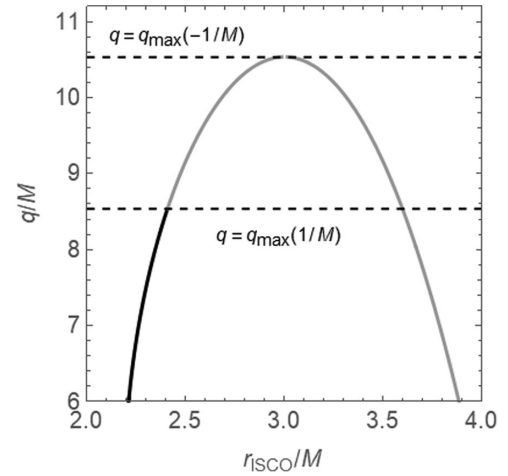FIG. 9. The inner and outer bands of stable circular orbits.

FIG. 10. The radius of the ISCO versus q for $b = 1/M$ (black) and $b = -1/M$ (gray). The gray curve is double valued in the interval $q_{max}(1/M) < q < q_{max}(-1/M)$ or $8.539M < q < 10.53M$.
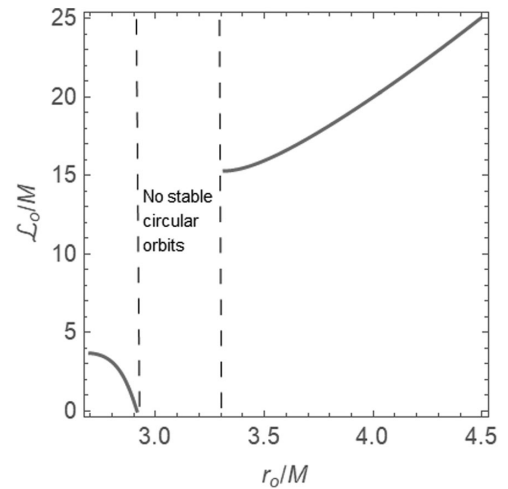

FIG. 11. The radius of the stable circular orbit r_o versus $\mathcal{L}_o$ when $b = -1/M$ and $q = 10M$. No stable circular orbits exist between the dashed lines.

(a) $b = \pm 0.02/M$.   (b) $b = \pm 0.1/M$.   (c) $b = \pm 1/M$.
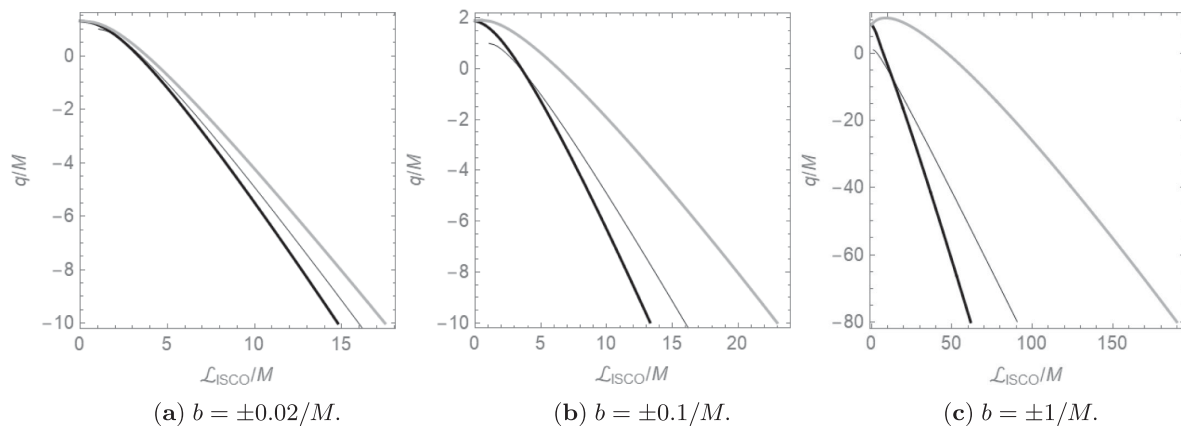
FIG. 12. The specific azimuthal angular momentum of a charged particle at the ISCO versus q for selected values of b. The thick black (gray) curve corresponds to the positive (negative) value of b. The thin curve corresponds to $b = 0$.

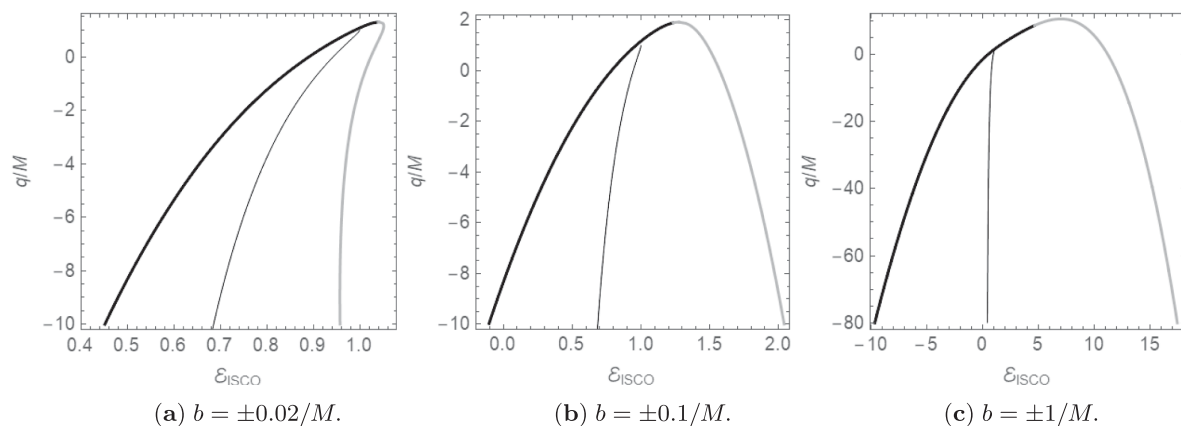(a) $b = \pm 0.02/M$.   (b) $b = \pm 0.1/M$.   (c) $b = \pm 1/M$.

FIG. 13. The specific energy of a charged particle at the ISCO versus q for selected values of b. The thick black (gray) curve corresponds to the positive (negative) value of b. The thin curve corresponds to $b = 0$.

at which $\mathcal{L}_o = 0$. The true ISCO is the inner ISCO. Figure 9 demonstrates this structure.

As an illustration, let us consider the case of Fig. 7(c), where $b = -1/M$. Figure 10 is a magnification of the region where two ISCOs exist in Fig. 7(c).

Figure 11 shows how the radius of the circular orbit r_o changes with $\mathcal{L}_o$ when $b = -1/M$ and $q = 10M$. The inner (true) ISCO is at $r_o = 2.682M$. Between $r_o = 2.914M$ (the value when $\mathcal{L}_o = 0$) and $r_o = 3.314M$ (the larger r_{ISCO}), no stable circular orbits exist.

Figures 12 and 13 show $\mathcal{L}_{\text{ISCO}}$ and $\mathcal{E}_{\text{ISCO}}$ that correspond to r_{ISCO} shown in Fig. 7. It is compelling that $\mathcal{E}_{\text{ISCO}}$ becomes negative when $b > 0$ after q falls behind a certain negative value, call it q_o. Figure 14 shows how q_o changes with b. The parameter q_o approaches 0 ($-\infty$) as b approaches ∞ (0). We can write approximate expressions for q_o when $b \ll 1/M$ or $b \gg 1/M$. They read

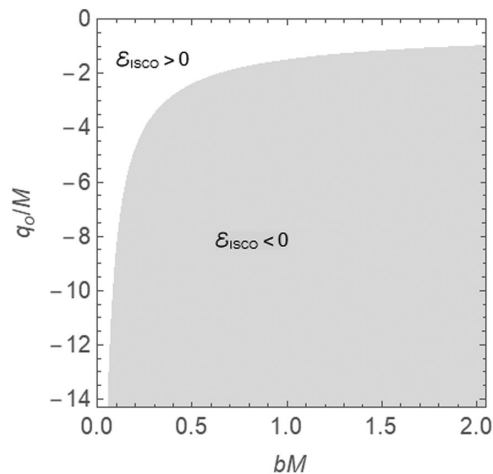$$q_o \approx -\sqrt{\frac{8\sqrt{3}M}{9b}} = -1.241\sqrt{\frac{M}{b}} \qquad (b \gg 1/M), \qquad (56)$$

FIG. 14. The critical charge parameter q_o at which $\mathcal{E}_{\text{ISCO}}$ vanishes versus b. For $q < q_o$ (gray region), $\mathcal{E}_{\text{ISCO}}$ is negative.

$$q_o \approx -\frac{1}{2b} \qquad (b \ll 1/M). \qquad (57)$$

This finding may have important astrophysical consequences. The energy liberated by a charged particle ending in such an ISCO can be several orders of magnitude greater than its rest energy. Similar "superbound" stable circular orbits were found near magnetized Kerr black holes in Ref. [20]. However, we are not aware of any negative-energy orbits outside the event horizon of the Schwarzschild black hole.

VII. SUMMARY

We have studied the ISCOs of charged particles near a weakly charged and magnetized Schwarzschild black hole. The effect of the black hole's charge alone is to push the ISCO beyond the neutral particle's ISCO, regardless of whether the Coulomb force is repulsive or attractive. When the Coulomb force is repulsive, the ISCO does not exist beyond some critical ratio of the Coulomb force to the "gravitational force." The binding energy of a charged particle at the ISCO can be as much as the particle's rest energy.

The effect of the magnetic field alone is to bring the ISCO closer than the neutral particle ISCO in all cases. When the magnetic force is radially out, the particle's ISCO can approach the event horizon where the particle's binding energy approaches its rest energy.

The problem becomes much richer when the black hole is both charged and magnetized. The charge and magnetic field have competitive effects on the ISCO's radius. The critical ratio of the Coulomb force to the gravitational force beyond which the ISCO does not exit becomes greater as the magnetic field becomes stronger. An interesting result is that the particle's energy can be negative. The energy liberation in such cases can be several orders of magnitude greater than the particle's rest energy.

The most interesting result is the possibility of the existence of two bands of charged particles' circular orbits, separated by a region of no stable circular orbits.

The problem can be more sophisticated and more astrophysically interesting when restudied in Kerr spacetime. The black hole rotation can have significant effects on the energy libation efficiency, position of the ISCOs and hence the forbidden zone. Another important modification is to consider more realistic magnetic fields.

ACKNOWLEDGMENTS

[1] C. W. Misner, K. S. Thorne, and J. A. Wheeler, *Gravitation* (W. H. Freeman and Co., San Francisco, 1973).

[2] M. Zajaek and A. Tursunov, arXiv:1904.04654.

[3] M. Zajaek, A. Tursunov, A. Eckart, S. Britzen, E. Hackmann, V. Karas, Z. Stuchlík, B. Czerny, and J. Anton Zensus, J. Phys. Conf. Ser. **1258**, 012031 (2019).

[4] M. Zajaek, A. Tursunov, A. Eckart, and S. Britzen, Mon. Not. R. Astron. Soc. **480**, 4408 (2018).

[5] B. Carter, in *Black Hole Equilibrium States, Black Holes*, edited by C. DeWitt and B. S. DeWitt (Gordon and Breach, New York, 1973), p. 57.

[6] R. M. Wald, Phys. Rev. D **10**, 1680 (1974).

[7] G. Romero and G. Vila, *Introduction to Black Hole Astrophysics* (Springer-Verlag, Berlin, 2013).

[8] B. Punsly, *Black Hole Gravitohydromagnetics*, 2nd ed. (Springer-Verlag, Berlin, 2008).

[9] Ruth A. Daly, Astrophys. J. **886**, 37 (2019).

[10] M. Yu. Piotrovich, Yu. N. Gnedin, N. A. Silant'ev, T. M. Natsvlishvili, and S. D. Buliga, Astron. Nachr. **336**, 1013 (2015).

[11] M. Y. Piotrovich, Y. N. Gnedin, S. D. Buliga, T. M. Natsvlishvili, N. A. Silant'ev, and A. I. Nikitenko, ASP Conf. Ser. **494**, 114 (2015), http://aspbooks.org/custom/publications/paper/494-0114.html.

[12] N. A. Silant'ev, Yu. N. Gnedin, S. D. Buliga, M. Yu. Piotrovich, and T. M. Natsvlishvili, Astrophys. Bull. **68**, 14 (2013).

[13] M. Yu. Piotrovich, N. A. Silantev, Yu. N. Gnedin, and T. M. Natsvlishvili, arXiv:1002.4948.

[14] L. Brenneman, *Measuring the Angular Momentum of Supermassive Black Holes*, Springer Briefs in Astronomy (Springer, New York, 2013).

[15] M. A. Abramowicz and P. C. Fragile, Living Rev. Relativity **16**, 1 (2013).

[16] M. A. Abramowicz, M. Jaroszyński, S. Kato, J.-P. Lasota, A. Różańska, and A. Sądowski, Astron. Astrophys. **521**, A15 (2010).

[17] D. V. Galtsov and V. I. Petukhov, Sov. Phys. JETP **47**, 419 (1978).

[18] A. N. Aliev and D. V. Gal'tsov, Sov. Phys. Usp. **32**, 75 (1989).

[19] A. N. Aliev and N. Özdemir, Mon. Not. R. Astron. Soc. **336**, 241 (2002).

[20] A. M. Al Zahrani, Phys. Rev. D **90**, 044012 (2014).

[21] D. Pugliese, H. Quevedo, and R. Ruffini, Eur. Phys. J. C **77**, 206 (2017).

[22] D. Pugliese, H. Quevedo, and R. Ruffini, Phys. Rev. D **83**, 104052 (2011).

[23] J. P. Hackstein and E. Hackmann, Gen. Relativ. Gravit. **52**, 22 (2020).